

Microstructure and Properties of 6061 Aluminum Alloy Brazing Joint with Al–Si–Zn Filler Metal

Wei Dai¹, Songbai Xue^{1,*}, Jiyuan Lou² and Shuiqing Wang²

¹College of Materials Science and Technology, Nanjing University of Aeronautics and Astronautics, Nanjing 210016, P. R. China

²Zhejiang Xinrui Welding Material Co., Ltd, Zhejiang, 312000, P. R. China

Ternary Al–Si–Zn filler metals were designed in order to join the 6061 aluminum alloy. The microstructure, phase constitution and fracture morphology of the brazed joint were investigated. Results of the microstructure observation showed that eutectoid $\alpha(\text{Al}) + \eta(\text{Zn})$, $\alpha(\text{Al})$ solid solution, as well as Si particles formed in the filler metal. The melting points of these filler metals are much lower than Al–12Si alloy. The $\eta(\text{Zn})$, $\alpha(\text{Al})$ solid solution, and the primary Si particles were found in the 6061 Al brazing seam when using Al–0.2Si–78Zn and Al–2Si–62Zn filler metal, while the Al–Si eutectic were found when using Al–6.5Si–42Zn alloy. Results also indicate that the tensile strength of the 6061 Al brazed joints using Al–0.2Si–78Zn, Al–2Si–62Zn and Al–6.5Si–42Zn is 101, 109, 129 MPa, respectively. The fracture morphology of the brazed joints showed intergranular fracture mode while some transgranular fracture could be found in the joint of Al–6.5Si–42Zn filler metal.
[doi:10.2320/matertrans.M2012110]

(Received March 22, 2012; Accepted May 22, 2012; Published August 25, 2012)

Keywords: 6061 aluminum alloys, brazing, aluminum–silicon–zinc filler metal, microstructure, property

1. Introduction

The 6000 series aluminum alloy are heat treatable and widely used in automotive industry due to their specific mechanical properties, corrosion resistance and formability.^{1,2)} Brazing of these alloys is often required to form a complex structure. Thought series of efforts have been made in the past few years, the problems of brazing these alloys still exist. L. C. Tsao *et al.*^{3,4)} developed a low-temperature Al–Si–20Cu-based filler metals, which the butt joint strength of 6061-T6 is about 200 MPa. But the brazing temperature is 873 K, too close to the solidus of 6061 alloy. A direct furnace solder with ultrasonic coating technique was introduced by Ding *et al.*⁵⁾ to solder the 6061 alloy, which the soldering temperature is about 533 K. However, the Pb in the solder do not confirm to the RoHS (The Restriction of the use of certain Hazardous substances in Electrical and Electronic Equipment) restriction.

Zinc filler is one of the oldest filler metal for join aluminum to aluminum at lower temperature. 1070 Al alloy could be soldered using Sn–xZn solders by ultrasonic soldering, and the relatively high strength joints could be obtained.⁶⁾ The wetting properties of the Zn–Al alloy on the alumina reinforced 6061 Al matrix composite surface were interested by Xu,⁷⁾ the research observed that the liquid filler could wet the oxidized substrate in air by undermining the substrate oxide layer. The researchers also found that the zinc could instead of 4XXX Al as a filler layer for aluminum brazing in composite brazing aluminum foil applications.⁸⁾ Actually, Zinc was also chosen as an important element in order to reduce the brazing temperature in Al–Si fillers,^{9,10)} 20% Zn addition to the Al–Si–Cu alloy could decrease the melting point to lower than 773 K. Add Zinc to the Al–Si alloy, could be an important part of the development of low-temperature aluminum filler metal.

The effect of this study is concerned with the applications for brazing 6061-T6 Al by the novel Al–Si–Zn filler metals at low-temperature. The characteristics of the filler metals were studied and the microstructures, elements distribution, tensile properties of the brazed joints were observed.

2. Materials and Experimental Procedure

The base metal was wrought aluminum alloy 6061-T6 plates with dimensions of 60 mm × 25 mm × 3 mm. The chemical compositions of the alloys are shown in Table 1. The preparation of the Al–Si–Zn filler metal was conducted in a crucible electrical resistance furnace at 1023 ± 10 K, then the melting filler metals were poured into a steel mould. The chemical compositions of the filler metals in the study were test by XRF spectrum analysis, and the results were also shown in Table 1. Differential thermal analysis was used to determine the melting temperature of the filler metals, which were heated from room temperature to 873 K under argon atmosphere at a heating rate of 10 K/min. Prior to brazing, the specimens and the filler metal were degreased in acetone and ground by SiC paper. It is well know that the magnesium element in 6061Al will diffuses out and forming a stable magnesium oxide which is difficult to removed during brazing. Therefore, a modified aluminum flux that includes Cs–Al–F compounds was applied for the purpose of oxide removal. The melting temperature of this flux is in the range of 733–823 K. Stable heating equipments with four torches

Table 1 Chemical composition of the alloys (mass%).

Alloy	Mn	Mg	Si	Cu	Cr	Al	Zn
6061-T6	0.01	1.10	0.61	0.25	0.12	Bal.	0.01
Filler metal 1	—	—	0.2	—	—	Bal.	77.6
Filler metal 2	—	—	2.0	—	—	Bal.	62.2
Filler metal 3	—	—	6.5	—	—	Bal.	41.8

*Corresponding author, E-mail: xuesb@nuaa.edu.cn

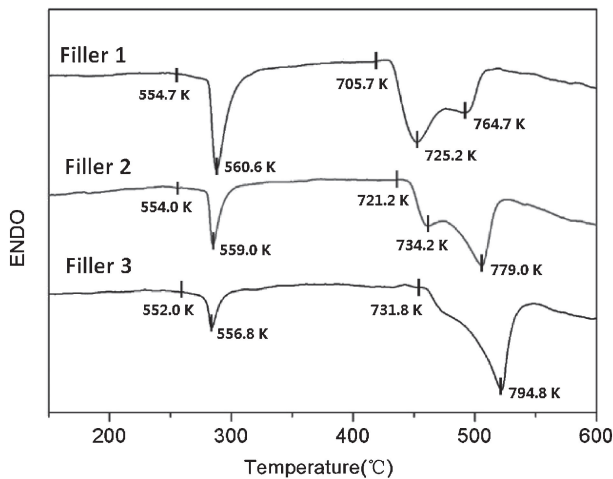


Fig. 1 DTA curve of the filler metals.

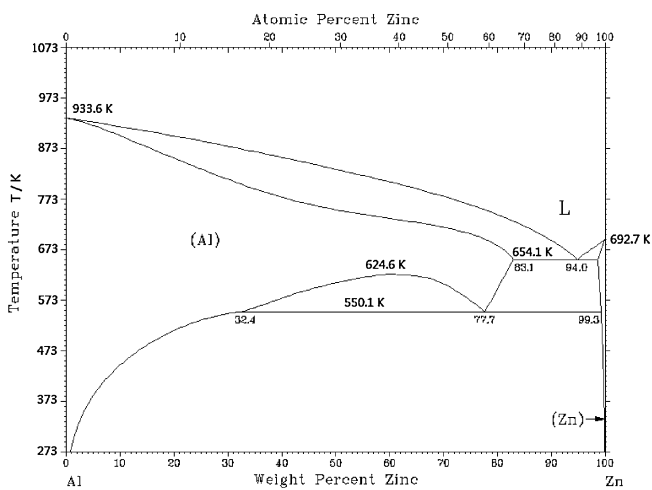


Fig. 2 Al-Zn equilibrium diagram.

were used in this experiment, the gas was controlled by the flow meter and the heating time was controlled by a automatic welding dolly.

The strength of brazed joints were tested on a SANS electromechanical universal testing system, and the average value of tested results were calculated and used. To ensure the accuracy of the results, five specimens were brazed at the same conditions with the same brazing alloy. The microstructures of the filler and joints were characterized by optical microscopy and field-emission scanning electron microscope coupled to energy dispersion X-ray (EDX).

3. Results and Discussion

3.1 Characteristics of the filler metals

Figure 1 shows the DTA curves of the filler metal 1 (Al-0.2Si-78Zn), filler metal 2 (Al-2Si-62Zn), and filler metal 3 (Al-6.5Si-42Zn). The peaks were all found at about 553 K in the three curves, from the Al-Zn equilibrium diagram (Fig. 2) the eutectoid reaction could be found at 550 K, and then the eutectoid $\alpha(\text{Al}) + \eta(\text{Zn})$ formed. The solidus and liquidus changes followed the composition of the filler metal. The operate window of filler metal 1 is about 90 K because the solidus of 6061 Al is about 855 K. The window is about

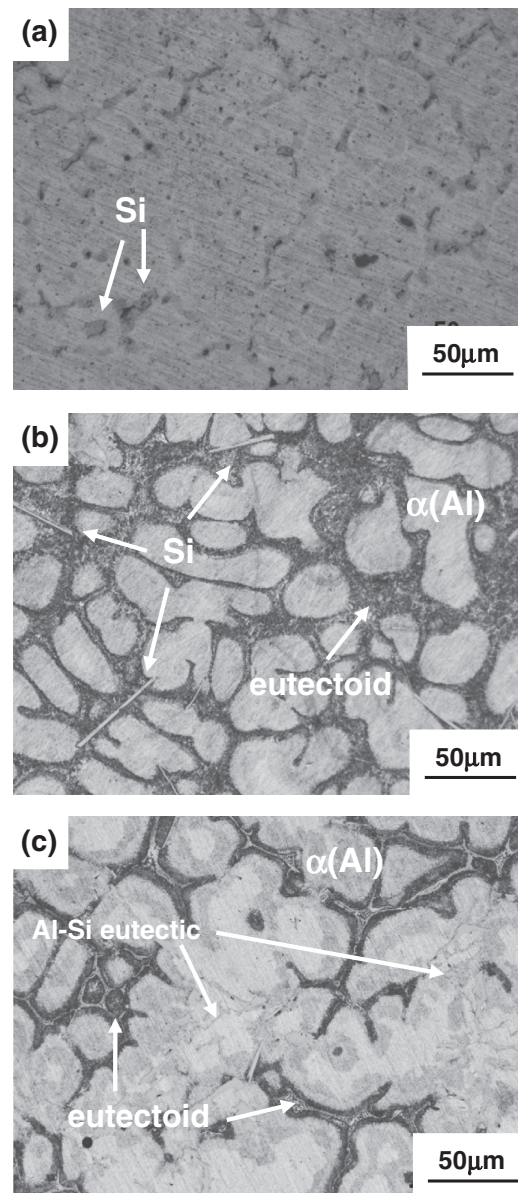


Fig. 3 Microstructure of the filler metals ((a) Filler metal 1. (b) Filler metal 2. (c) Filler metal 3).

60 K when using filler metal 3, which is much larger than that of the typically Al-12Si filler metal (about 5 K). The brazing temperature too close to the melting point of the Al workpieces could increase the filler metal penetration into the base metal and cause erosion, results in distortion of the brazed part. The lower melting point filler metal is helpful to decrease this harmful phenomenon. Meanwhile, the melting point of the non-corrosive flux in this research is about 733 K, these three type of filler metal is very suitable for work with this flux.

The microstructures of the filler metals could be seen in Fig. 3, when the compositions changes in the filler metal, the microstructures changes obversely. The small silicon particles evenly dispersed in the Al-0.2Si-78Zn alloy, as shown in Fig. 3(a). However, needlelike primary silicon phases were found when the Si content is 2.0 mass% while the reticular Si phase formed when the Si content reaches 6.5 mass%. Si could react with Al to form Al-Si eutectic, but seldom Si

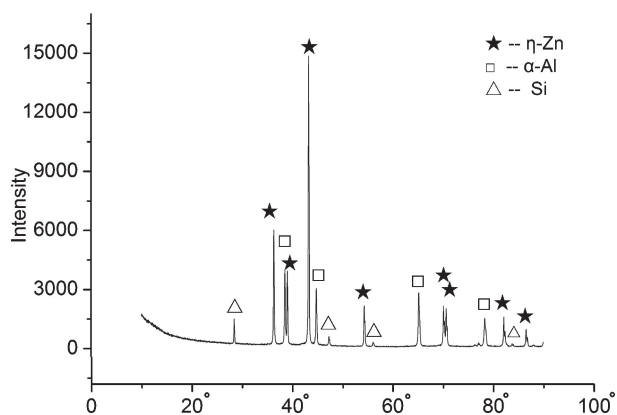


Fig. 4 XRD pattern of filler metal 3.

could resolve in Zn from Zn–Si equilibrium diagram, meanwhile, Zn–Al–Si could not form the ternary compound. So the dark phase surround $\alpha(\text{Al})$ in Figs. 3(b) and 3(c) may be the eutectoid $\alpha(\text{Al}) + \eta(\text{Zn})$. From the XRD pattern of filler metal 3 (Fig. 4), the $\alpha(\text{Al})$, $\eta(\text{Zn})$ and the Si phases could all be found, by the analyze above, the phases in the filler metal are $\alpha(\text{Al})$, eutectoid $\alpha(\text{Al}) + \eta(\text{Zn})$, Al–Si eutectic as well as the Si particles.

3.2 Microstructure of the 6061 Al brazed joints

Figure 5 shows the microstructure of the 6061 Al brazing seams using filler metals 1, 2 and 3, sound joints could be obtained. The bamboo shoot-like solid solutions were formed at the interface of the joint, this type of solid solutions is helpful for improve the strength of the joints. The Si particles distributed finely in the brazing seam, and in the brazing seam of filler metal 3, both the primary silicon and the Al–Si eutectic were found.

To understand the phase construction of the brazing seam by filler 2, the large magnification picture were obtained (Fig. 6). From the result list in Table 2, the content of Al in the brazing seam is much higher than the filler (36 mass%), show that Al dissolution from base metal into the filler and formed these supersaturated solid solution phases. The white phase B in Fig. 6 consists of about 97 mass% Zn, Movahedi⁸⁾ thought it is a solid solution phase. But in Movahedi's study, the pure zinc was used as the filler metal, using filler 2, this zinc rich phase could also formed after brazing. Dong¹¹⁾ reported that a cermet composite consisting of a ZnO network embedded in a Zn–Al matrix when using ZnAl alloy weld the 5A02 Al to stain steel by gas–tungsten arc welding. The ZnO network structure were formed by the reaction of oxygen on the stainless steel surface and liquid zinc, and upon cooling, some ZnO arms grew upward into the weld and broke down into strips or islands. But in this study, no oxygen were found in the zinc rich phase, the flux used when brazing could remove the oxide on the Al surface and keep the wetting interface isolated from the oxygen in the air. By the results above and the Al–Zn equilibrium diagram, this white phase may be $\eta(\text{Zn})$ phase.

Movahedi *et al.*⁸⁾ did not find the evidence of eutectoid phase formation in the microstructures of the brazing seam, and the absence of eutectoid phases may be related to the nonequilibrium solidification during brazing. But from the

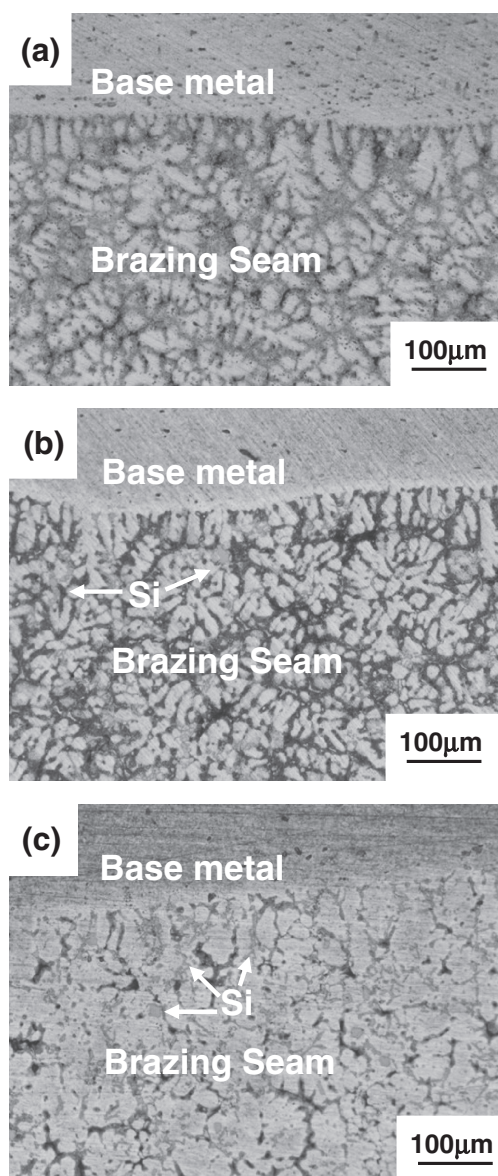


Fig. 5 Microstructure of the 6061 Al brazing seam ((a) Filler metal 1, (b) Filler metal 2, (c) Filler metal 3).

EDX result of area C in Fig. 6, we found this area with 65.97 mass% zinc and 34.03 mass% aluminum which is close to the eutectoid area. In as-cast ZA48 alloys, Yan *et al.*¹²⁾ found the eutectoid $\eta(\text{Zn}) + \alpha(\text{Al})$ surround with the primary α -dendrites structure, but they did not report the element distribution. By the content rate of zinc and aluminum, area C may be the eutectoid $\eta(\text{Zn}) + \alpha(\text{Al})$ phase and it formed surround the $\eta(\text{Zn})$ phase. Area D is $\alpha(\text{Al})$ from the result list in Table 2, the content of Al in the brazing seam is much higher than the filler (36 mass%), show that Al dissolution from base metal into the filler and formed these supersaturated solid solution phases. The diffusion of the aluminum and zinc to each other is helpful for the joint strength due to solid solution hardening.

Some micro-cracks were found on the Si particles, as showed in Fig. 7, and these micro-cracks may be the initiate crack of the joint when bear the force. Because of the difference of the thermal expansion coefficient between Si

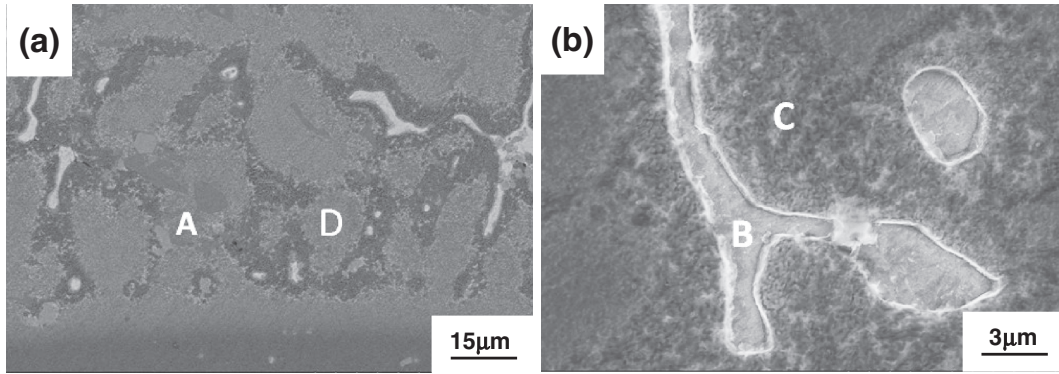


Fig. 6 SEM observations of 6061 Al brazing joint using filler metal 2 ((a) interface, (b) brazing seam).

Table 2 Composition and possible phase of the brazing seam.

Measure point	Element (mass%)			Possible phase
	Zn	Al	Si	
A	—	3.39	96.61	Si
B	96.81	3.19	—	$\eta(\text{Zn})$
C	65.97	34.03	—	$\eta(\text{Zn}) + \alpha(\text{Al})$
D	33.20	66.80	—	$\alpha(\text{Al})$

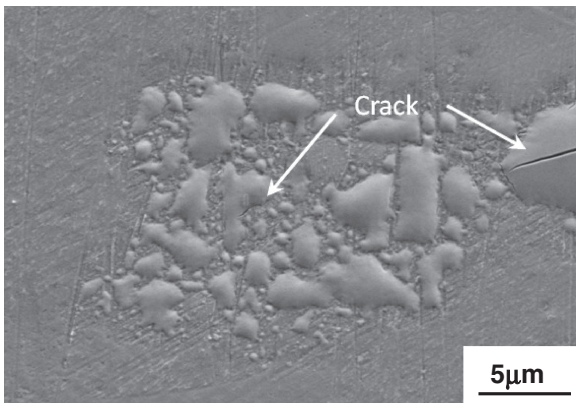


Fig. 7 Si particles in the brazing seam.

phase and the solid solutions, these micro-cracks may be formed by thermal shrinkage stress of the joint when cooling. The larger the Si phase, the easier cracks would form. From the XRD patterns of the brazing seam (Fig. 8), the brazing seams contained $\eta(\text{Zn})$, $\alpha(\text{Al})$ and Si phase. With the increasing of Al content in the filler metal, the diffraction peaks of $\eta(\text{Zn})$ decrease.

3.3 Tensile strength of the brazed joints

Figure 9 summarizes the tensile strength of the joints brazed by the three filler metals. The results indicated that the strength of the brazed joints are much different regarding to the filler metal. The 6061Al joint of filler 3 shows the highest value-129 MPa while the joints of filler 1 and 2 is 101 and 109 MPa, which means the higher content of Al in the brazing alloy are beneficial to increase the strength of the joints. From the strength of the joints we could also found that thought more silicon particles formed in the brazing seam of filler 3, the tensile strength did not decrease compare

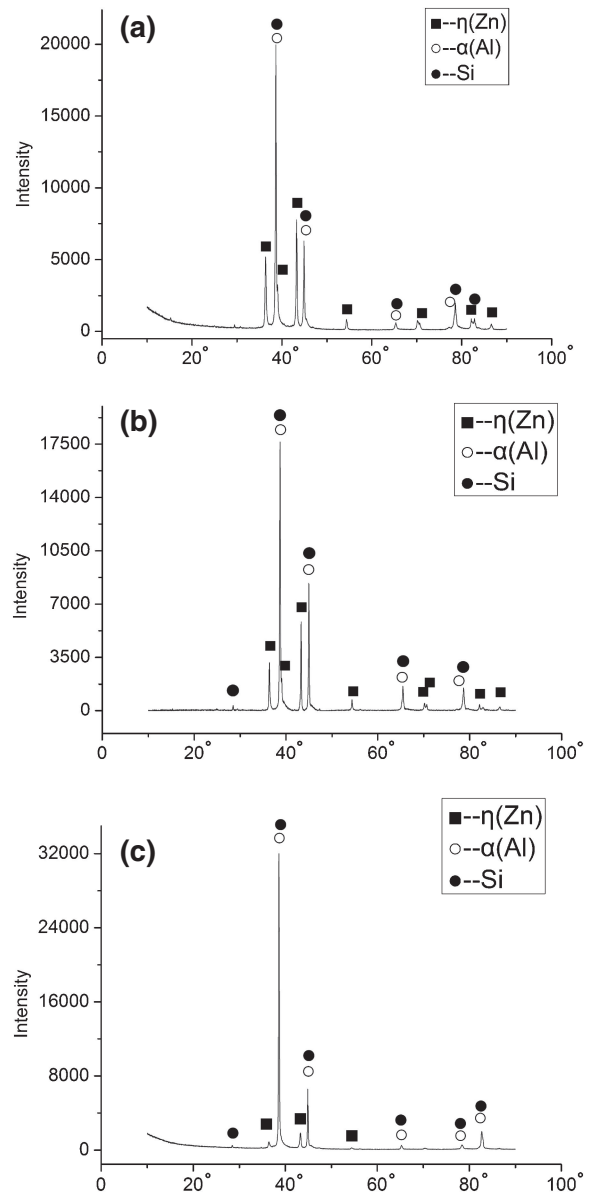


Fig. 8 XRD pattern of 6061 Al brazing seam ((a) filler 1, (b) filler 2, (c) filler 3).

to the filler 1 joints. The higher Al content in filler metal, the higher strength of the 6061 Al brazed joint, this tendency is similar as the research result by Liu,¹³⁾ as the Mg content in the filler increased, the tensile-shear strength of the AZ31

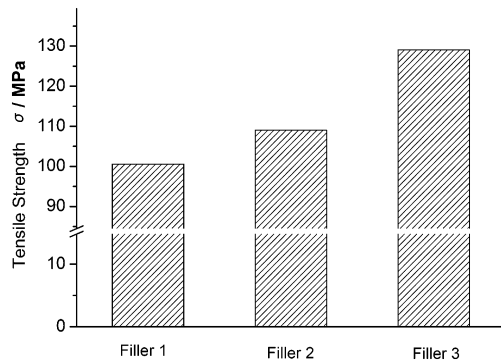


Fig. 9 Tensile strength of the 6061 Al brazed joints.

brazing joint increased from 30 MPa to more than 50 MPa. Meanwhile, the Zn and Al have a large solid solubility in each other, and Si could also solution in the $\alpha(\text{Al})$ solid solutions, which could increase the joint strength by solid solution hardening.¹⁴⁾

3.4 Typical fracture of the brazed joints

Typical fracture morphologies of 6061 Al joints (joint 1, 2, 3) brazed by filler metal 1, 2, 3 are shown in Fig. 10, they all showing the brittle fracture pattern. The fracture of the brazed joint exhibits intergranular fracture in joint 1 and 2, and micro cracks can be seen in the fracture. Some of the transgranular fracture could be found in joint 3, and the Si particles may fall off the fracture when tensile from Fig. 10(c). These Si particles in the brazing seam is similar like the intermetallic brittle compounds, which could deteriorate the tensile property of the joint.^{15,16)} The phase could be optimized by control the cooling rate¹⁷⁾ and the alloying method.¹⁸⁾ Because of the Al content in filler metal 3 is much higher than filler 1 and 2, more $\alpha(\text{Al})$ formed in the brazing joint 3, the $\alpha(\text{Al})$ greatly increased the tensile strength of the 6061Al brazing joint.

4. Summary and Conclusion

The research developed a series of economic and available Al-Si-Zn filler metals to join 6061 aluminum, the following conclusions could be obtained:

- (1) The Al-Si-Zn series filler metals with a liquidus around 500°C could successfully used for braze the 6061 Al. The small primary silicon particles could be found in Al-0.2Si-78Zn filler metal while the needlelike primary silicon particles could be found in the filler metal while the Si content is 2.0%. Meanwhile, the Al-Si eutectic could be found in the Al-6.5Si-42Zn filler metal.
- (2) The eutectoid $\alpha(\text{Al}) + \eta(\text{Zn})$, $\alpha(\text{Al})$, $\eta(\text{Zn})$ as well as the Si particles could also be found in the brazing seam. The Al-Si eutectic could be found when using Al-6.5Si-42Zn filler metal. Some micro-cracks formed in the Si particles could be the crack source of the brazed joint.
- (3) The tensile strength of the Al-6.5Si-42Zn brazed joints could achieve 129 MPa. The fracture morphologies of the joints exhibits intergranular fracture while some transgranular fracture could be found in Al-6.5Si-42Zn joint.

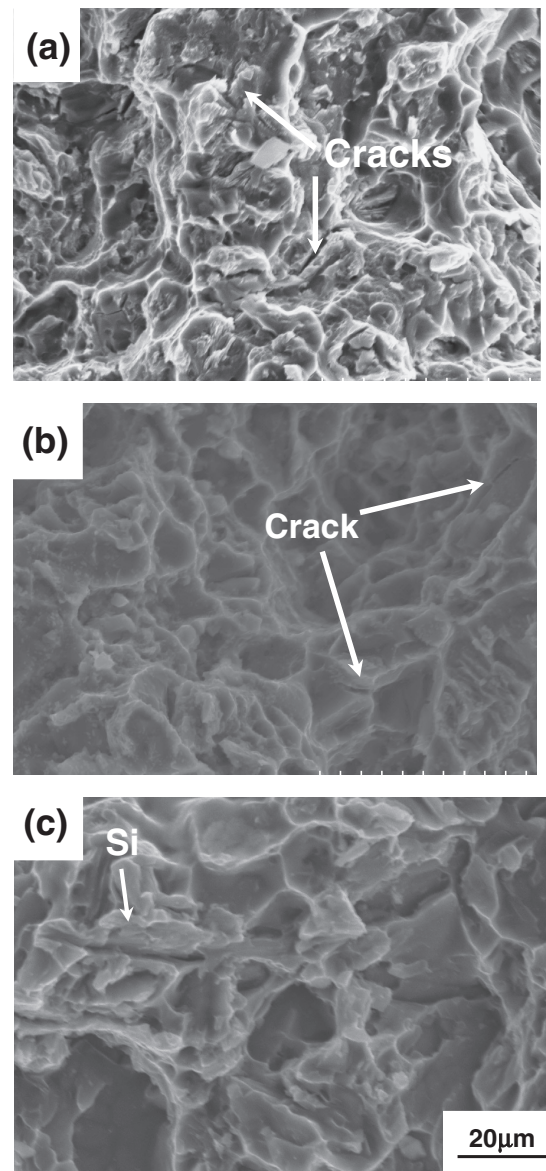


Fig. 10 Typical fracture morphology of 6061 Al brazed joints ((a) filler 1, (b) filler 2, (c) filler 3).

Acknowledgements

The project is supported by the Foundation of Scientist and Technician Serve the Enterprise, The Ministry of Science and Technology, China (Project No. 2009GJC20040).

REFERENCES

- 1) W. S. Miller, L. Zhuang and J. Botema: *Mater. Sci. Eng. A* **280** (2000) 37-49.
- 2) O. Engler and J. Hirsch: *Mater. Sci. Eng. A* **336** (2002) 249-262.
- 3) L. C. Tsao, T. C. Tsai, C. S. Wu and H. T. Chuang: *J. Mater. Eng. Perform.* **10** (2001) 705-709.
- 4) S. Y. Chang, L. C. Tsao, T. Y. Li and H. T. Chuang: *J. Alloy. Compd.* **488** (2009) 174-180.
- 5) M. Ding, P. L. Zhang, Z. Y. Zhang and S. Yao: *Ultrason. Sonochem.* **17** (2010) 292-297.
- 6) T. Nagaoka, Y. Morisada, M. Fukusumi and T. Takemoto: *J. Mater. Process. Tech.* **209** (2009) 5054-5059.

- 7) Z. W. Xu, J. C. Yan, G. H. Wu, X. L. Kong and S. Q. Yang: *Compos. Sci. Technol.* **65** (2005) 1959–1963.
- 8) M. Movahedi, A. H. Kokabi and H. R. Madaah Hosseini: *Mater. Charact.* **60** (2009) 441–446.
- 9) L. C. Tsao, M. J. Chiang, W. H. Lin, M. D. Cheng and T. H. Chuang: *Mater. Charact.* **48** (2002) 341–346.
- 10) K. Suzuki, M. Kagayama and Y. Takeuchi: *Light Metal* **43** (1993) 533–538.
- 11) H. Dong, L. Yang, C. Dong and S. Kou: *Mater. Sci. Eng. A* **527** (2010) 7151–7154.
- 12) S. Yan, J. Xie, Z. Liu, J. Li, W. Wang and A. Wang: *J. Mater. Sci.* **44** (2009) 4169–4173.
- 13) L. M. Liu and Z. H. Wu: *Mater. Charact.* **61** (2010) 13–18.
- 14) L. Ma, D. Y. He, X. Y. Li and J. M. Jiang: *Mater. Lett.* **64** (2010) 596–598.
- 15) M. Ghosh and S. Chatterjee: *Mater. Charact.* **54** (2005) 327–337.
- 16) P. He and D. Liu: *Mater. Sci. Eng. A* **437** (2006) 430–435.
- 17) M. A. Mofid, A. Abdollah-zadeh and F. M. Ghaini: *Mater. Design* **36** (2012) 161–167.
- 18) Y. Shi, Y. Yu and Y. Li: *J. Mater. Eng. Perform.* **18** (2009) 278–281.